Deep Brain Stimulation for Depression Informed by Intracranial Recordings

Supplementary Information

Clinical Trial

This is an early feasibility trial (NCT03437928) focused on patients with treatment-resistant depression (TRD). Inclusion criteria consist of failure of conventional therapies (pharmacological, cognitive/behavioral, electroconvulsive), severity of symptoms, and ability to provide informed consent, among others. Exclusion criteria include history of psychosis, personality disorder, recent suicide attempt, or neurodegenerative disorder. This trial is funded by the NIH BRAIN Initiative (UH3 NS103549) and approved by the FDA (IDE number G180300) and our multi-center IRB (Baylor College of Medicine IRB number H-43036).

The overall structure of the trial begins with surgical implantation of 4 DBS leads (bilateral SCC and VC/VS) as well as 10-12 sEEG electrodes in frontotemporal areas as shown in Figure 1. We then perform 9 days of recording and stimulation in the NMU through the externalized DBS leads and sEEG electrodes, followed by return to surgery for removal of the sEEG electrodes and internalization of the DBS leads to two pulse generators. DBS stimulation is initiated 2 weeks later, using parameter sets generated from the NMU-derived data. After apprxomately 8 months of this open-label stimulation, the subject enters the final phase of the trial, randomized and blinded discontinuation. For each subject, we randomly choose which DBS pair to taper during the first discontinuation (this first subject was randomized to SCC). Only the unblinded programmer is aware of this choice. Stimulation amplitude is reduced by 25% during each weekly visit in double-blinded fashion. If the subject's symptoms worsen and meet escape

criteria (see caption of Figure 2B), they are reinstated to full stimulation and exited from the discontinuation phase (the other DBS target pair is not tapered to reduce risk). If symptom severity does not worsen to meet escape criteria, the other DBS target pair is tapered in the same way. A subject entering the discontinuation phase as a responder (>50% reduction in MADRS) whose severity does not increase to escape criteria during discontinuation of both DBS targets would be considered to have a sham response. On the other hand, a responder who worsens during blinded tapering (as in this subject) would be considered to have a true response.

Trajectory Planning

DBS targets were planned using previously described methodology on patient-specific diffusion-weighted imaging data (1). Leads were positioned to span the region of SCC and VC/VS with the joint maximal probability of connectivity with white matter tracts critically associated with each respective target, herein referred to the tractography-optimized target (TOT). For SCC, we optimized the position with respect to connectivity with forceps minor, cingulum, uncinate fasciculus, and tracts to ventral striatum; for VC/VS, we targeted the subregion maximally connected to dorsolateral prefrontal cortex, nucleus accumbens, amygdala, medial and lateral orbitofrontal cortex. The VC/VS trajectory was also designed to be inclusive of the recently described consensus OCD target tracts (2) as well as previously described anatomic targets. For each of the four trajectories, we planned to place the lower segmented level of the DBS lead (contacts 2-3-4) at target in order to maximize the potential of directional current steering.

The sEEG electrodes were planned to span regions of dorsolateral prefrontal cortex (dlPFC), ventrolateral prefrontal cortex (vlPFC), orbitofrontal cortex (OFC), ventromedial

prefrontal cortex (vmPFC), anterior cingulate cortex (ACC), and medial temporal lobe, based on patient-specific tractography as defined by TOT connectivity as well as atlas-based tractography. These regions were chosen because of their known involvement in the mood, affect, and cognitive dysfunction characteristic of TRD (3, 4).

Three-dimensional holographic planning (Figure 1A) was performed using custom software ("HoloSEEG") running on the Microsoft HoloLens. The literature has discussed the relative merits and risks of using individual vs. group diffusion data in tractographic analyses (5-7). Disadvantages of the former include low signal to noise, whereas disadvantages of the latter include blurring of inter-individual differences. We favored emphasizing the individual-specific information while trying to mitigate signal-to-noise limitations by imposing anatomically known constraints on the data during the planning process (8).

Surgical Procedure

The initial surgery consisted of implanting 10 sEEG electrodes (5 per hemisphere in the prefrontal and mesial temporal regions described above) and 4 DBS leads (VC/VS and SCC bilaterally). We used a stereotactic robot (ROSA, Zimmer Biomet) for the placement of the DBS leads and sEEG electrodes. We used segmented DBS leads that allow directional steering (Cartesia, Boston Scientific).

We first implanted the sEEG electrodes (Depthalon, PMT Corporation) using standard percutaneous techniques. We then made a single coronally oriented incision for the 4 separate burr holes for the 4 DBS leads. We placed the VC/VS leads with the patient awake, in order to test for the presence of a "mirth" or "positive valence" response, which may have predictive value for clinical improvement (9). We did elicit such a response in this target, with the subject

describing reduced anxiety and increased energy, with a subjective description of feeling "more online". We did not perform intraoperative stimulation testing of the SCC leads. The leads were connected to extensions, which were tunneled out through separate small incisions.

The second surgical procedure, following the NMU monitoring, consisted of removing the sEEG electrodes and internalizing new DBS lead extensions to two implanted pulse generators (IPGs) in the bilateral upper chest.

NMU Recordings and Stimulation

The sEEG electrodes and DBS lead extensions were connected to a recording system (Blackrock Microsystems) in the neurophysiological monitoring unit (NMU). Electrophysiological data were recorded at 2 kHz.

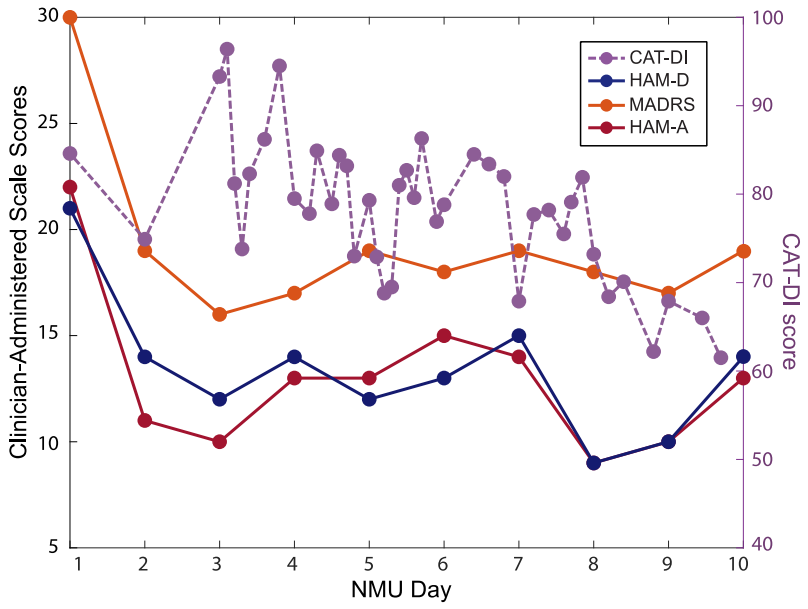

Figure S1. Evolution of clinical scores in the NMU. During the 9-day NMU stay, we performed standard clinician-administered scales (HAM-D, HAM-A, MADRS; primary y-axis) daily, and the rapidly assessed CAT-DI (secondary y-axis) up to several times per day. Symptom scores decreased over the course of the stay, reaching their minimum on the last two days. Day 10 is the day of the second surgery.

During the subject's stay in the NMU, we acquired the daily clinician-administered 17-item Hamilton Depression Rating Scale ($HAM\text{-}D_{17}$) and Montgomery-Asberg Depression Rating Scale (MADRS). We also incorporated time-resolved assessments of mood and affect, including the computerized adaptive test depression inventory (CAT-DI), a validated tool requiring only minutes to administer and therefore allowing much more frequent assessments (10) (Figure S1). A second time-resolved behavioral measure employed was the automated facial affect recognition (AFAR) system, which uses machine learning strategies on high-resolution videos to identify changes in facial 'action units' and thereby provides a continuous measures of a variety of affective states, such as positive affect, fear, disgust, and others (11).

We delivered stimulation time-locked with electrophysiological and behavioral recordings (Cerestim, Blackrock Microsystems).

Generation of Imaging Defined Parameter Set

We created SFMs using Brainlab software in patient-specific MRI space. For each DBS lead, we used 7 contact configurations corresponding to the 4 "ring" configurations in each of the 4 levels and the 3 vertical "stack" configurations in the 2 segmented levels (see Figure 2A part 1 for a visualization of the contact arrangement for this lead). Finally, for each of the 7 contact configurations per lead, we defined an SFM for each combination of amplitude (2, 5mA) and pulse width (50, 100, 180 μs). After the linear registration ('flirt' function in fsl) (12) of the TOT to the patient-specific imaging space, we calculated the intersection between the SFMs and the TOT area and retrieved the volume (mm^3) of overlap (Figure S2). The imaging defined parameter set was chosen as the parameter combination (per lead) resulting in greatest overlap.

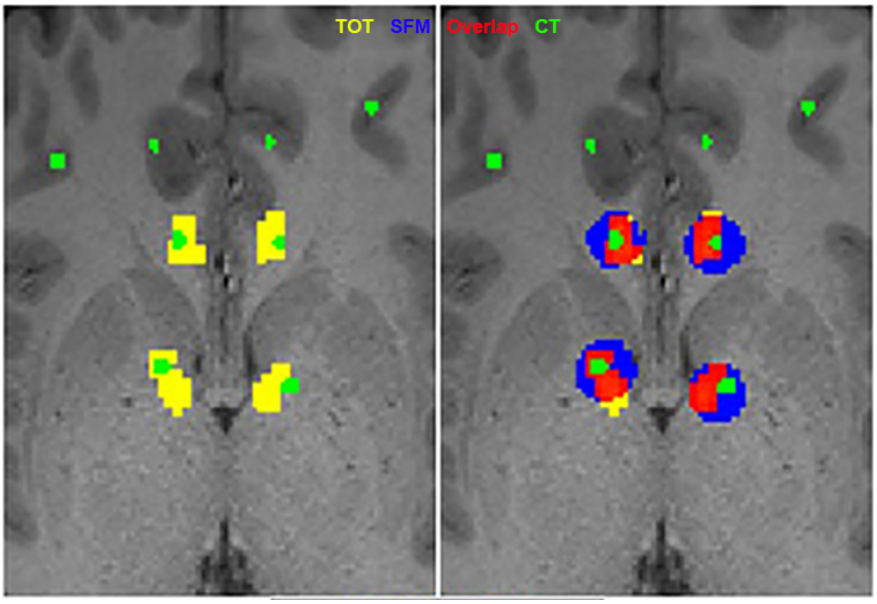

Figure S2. Generation of Imaging Defined Parameter Set. Left panel: CT and sEEG electrodes are shown in green. The tractography optimized target (TOT) for both SCC and VC/VS DBS targets is shown in yellow. Right panel: The blue regions are SFMs for a particular stimulation parameter set, and their overlap with the TOT is shown in red.

Generation of Electrophysiologically Defined Parameter Set

We used the 1 second stimulation data to generate the electrophysiologically defined parameter set. We tested a wide range of parameter space by varying frequency (6, 50, 130 Hz), amplitude (2, 5 mA), and pulse width (50, 100, 180 microsec). We also varied the contact configuration by separately testing the bottom bullet-shaped contact, top ring contact, and three "stacks" of segmented contacts in the middle two levels on the VCVS leads (5 total configurations). For the SCC leads we additionally tested the middle two segmented levels (7 total configurations). We tested all combinations of these parameters across the four leads, for a total of 432 sets. We repeated each 10 times with an 8 second inter-trial interval (ITI).

Data were analyzed (Matlab) from a 6-second window from the ITI period to avoid stimulation artifact (2-8 seconds from stimulation onset). sEEG electrode data were notch-

filtered to remove line noise (60, 120, and 180 Hz), decimated from 2kHz to 500 Hz sampling rate, and referenced by subtracting mean activity from adjacent contacts along the sEEG probe. Theta- (4-7 Hz) and alpha-band (8-12 Hz) power was calculated for each channel by first band-pass filtering the data and then applying a Hilbert transformation to extract signal power. Each stimulation parameter set was thus associated with a 3D matrix of power across all 148 sEEG contacts across the canonical frequency bands (theta: 4-7 Hz, alpha: 8-12 Hz). Variance across stimulation parameters was calculated for each channel independently. Channels with the lowest variance across stimulation parameters were excluded from analysis (bottom quartile). Posthoc observations suggest high overlap of white matter channels and channels with low signal variance. To avoid an arbitrary cutoff, future implementations will exclude white matter channels.

The primary "desired" state, was defined in the same way using the 5 minutes eyes-open baseline rest period acquired on day 9, and the "undesired" state as the same on day 2 (Figure S3A). The alternate "desired" state was defined based on activity evoked by a positive mood-inducing task (Figure S3B). The subject watched short videos selected from a previously validated library (13). Data were analyzed (Matlab) from a 6-second window from the ITI period to avoid stimulation artifact (2-8 seconds from stimulation onset).

Stereo-EEG electrode data were notch-filtered to remove line noise (60, 120, and 180 Hz), decimated from 2kHz to 500 Hz sampling rate, and referenced by subtracting mean activity from adjacent contacts along the sEEG probe. Theta- (4-7 Hz) and alpha-band (8-12 Hz) power was calculated for each channel by first band-pass filtering the data and then applying a Hilbert transformation to extract signal power.

When treating the desired state as the resting-state data from Day 9, the range of correlation coefficients across all stimulation parameter combinations on all leads was 0.57 to 0.95. Left SCC, for example, had a range of 0.68 to 0.95 with a mean of 0.83 and a standard deviation of 0.06. The other leads had similar results – Right SCC had a range from 0.61 to 0.95; Left VC/VS had a range of 0.57 to 0.93; Right VC/VS had a range of 0.70 to 0.93. The final configuration of this parameter set was: Left SCC contacts 3-6, 3.5 mA, 180 us, 130 Hz; Right SCC contacts 5-6-7, 5.5 mA, 180 us, 130 Hz; Left VC/VS contact 1, 5.5 mA, 180 us, 130 Hz; Right VC/VS contacts 5-6-7, 4.5 mA, 180 us, 130 Hz.

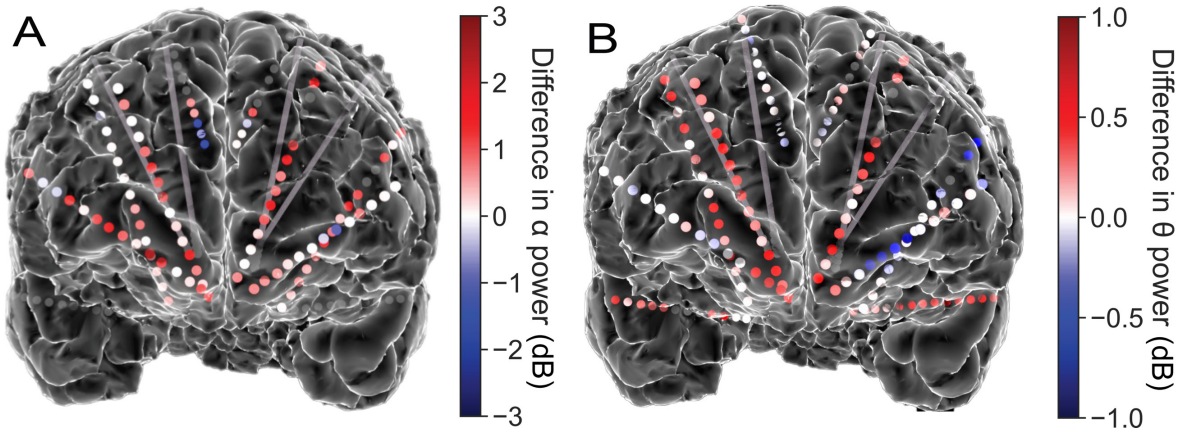

Figure S3. Network effects of varying mood states. A) Difference in alpha power between recordings during highest (on Day 9) and lowest (Day 2) mood state, as measured by CAT-DI (higher power in red). **B)** Difference in theta power between mood induced by positive and negative video stimuli (greater power during positive videos in red).

Figure S4 shows the stimulation parameters of the electrophysiologically defined parameter set compared to the other parameter sets generated by conventional methods. In particular, we generated an "imaging defined" parameter set (described above) and a "behaviorally defined" parameter set, based on subject responses to longer stimulation trains (15 sec, 5 minute, and 20 minute). The different parameters, especially contact configurations, suggest that these different methods can produce different results. We emphasize that this trial is

not designed to test these different methods head-to-head to determine optimality, but rather to demonstrate the novel concept of inverse programming based on electrophysiologically determined parameters. Thus the three parameter sets in Figure S4 are presented for illustrative purposes only.

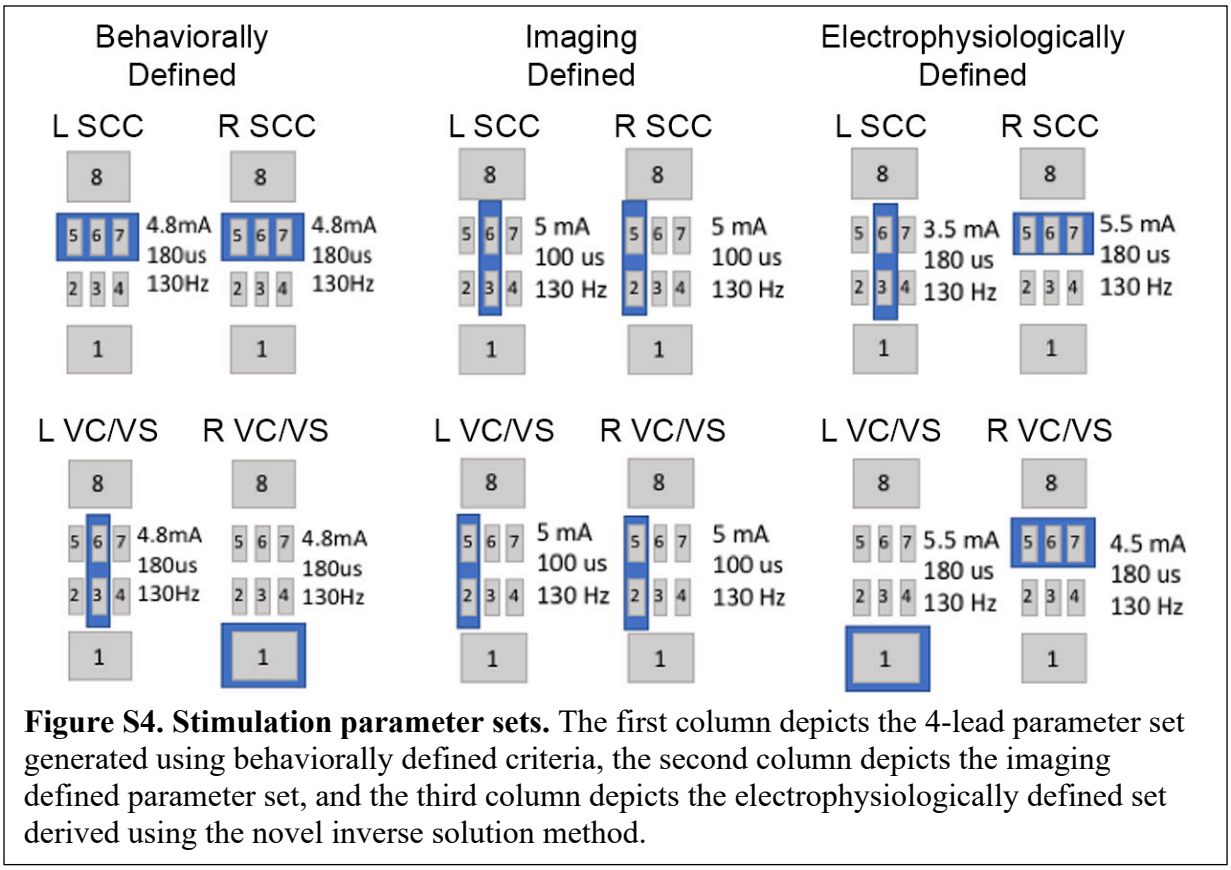

Figure S4. Stimulation parameter sets. The first column depicts the 4-lead parameter set generated using behaviorally defined criteria, the second column depicts the imaging defined parameter set, and the third column depicts the electrophysiologically defined set derived using the novel inverse solution method.

Supplementary References

1. Tsolaki E, Espinoza R, Pouratian N (2017): Using probabilistic tractography to target the subcallosal cingulate cortex in patients with treatment resistant depression. *Psychiatry Res Neuroimaging*. 261:72-74.
2. Li N, Baldermann JC, Kibleur A, Treu S, Akram H, Elias GJB, et al. (2020): A unified connectomic target for deep brain stimulation in obsessive-compulsive disorder. *Nat Commun*. 11:3364.
3. Drysdale AT, Grosenick L, Downar J, Dunlop K, Mansouri F, Meng Y, et al. (2017): Resting-state connectivity biomarkers define neurophysiological subtypes of depression. *Nat Med*. 23:28-38.
4. Williams LM (2016): Precision psychiatry: a neural circuit taxonomy for depression and anxiety. *Lancet Psychiatry*. 3:472-480.
5. Baldermann JC, Schuller T, Kohl S, Voon V, Li N, Hollunder B, et al. (2021): Connectomic Deep Brain Stimulation for Obsessive-Compulsive Disorder. *Biol Psychiatry*.
6. Wang Q, Akram H, Muthuraman M, Gonzalez-Escamilla G, Sheth SA, Oxenford S, et al. (2021): Normative vs. patient-specific brain connectivity in deep brain stimulation. *Neuroimage*. 224:117307.
7. Widge AS, Zhang F, Gosai A, Papadimitrou G, Wilson-Braun P, Tsintou M, et al. (2021): Patient-specific connectomic models correlate with, but do not reliably predict, outcomes in deep brain stimulation for obsessive-compulsive disorder. *Neuropsychopharmacology*.
8. Haber SN, Liu H, Seidlitz J, Bullmore E (2021): Prefrontal connectomics: from anatomy to human imaging. *Neuropsychopharmacology*.
9. Haq IU, Foote KD, Goodman WG, Wu SS, Sudhyadhom A, Ricciuti N, et al. (2011): Smile and laughter induction and intraoperative predictors of response to deep brain stimulation for obsessive-compulsive disorder. *Neuroimage*. 54 Suppl 1:S247-255.
10. Gibbons RD, Weiss DJ, Pilkonis PA, Frank E, Moore T, Kim JB, et al. (2012): Development of a computerized adaptive test for depression. *Arch Gen Psychiatry*. 69:1104-1112.
11. Ertugrul IO, Jeni LA, Ding W, Cohn JF (2019): AFAR: A Deep Learning Based Tool for Automated Facial Affect Recognition. *Proc Int Conf Autom Face Gesture Recognit*. 2019.
12. Jenkinson M, Bannister P, Brady M, Smith S (2002): Improved optimization for the robust and accurate linear registration and motion correction of brain images. *Neuroimage*. 17:825-841.
13. Samide R, Cooper RA, Ritchey M (2020): A database of news videos for investigating the dynamics of emotion and memory. *Behav Res Methods*. 52:1469-1479.